

Rare top decays $t \rightarrow c\gamma$, $t \rightarrow cg$ and CKM unitarity

J. A. Aguilar-Saavedra and B. M. Nobre

Departamento de Física and Grupo de Física de Partículas (GFP),

Instituto Superior Técnico, P-1049-001 Lisboa, Portugal

Abstract

Top flavour-changing neutral decays are extremely suppressed within the Standard Model (SM) by the GIM mechanism, but can reach observable rates in some of its extensions. We compute the branching ratios for $t \rightarrow c\gamma$ and $t \rightarrow cg$ in minimal SM extensions where the addition of a vector-like up or down quark singlet breaks the unitarity of the 3×3 Cabibbo-Kobayashi-Maskawa (CKM) matrix. The maximum rates obtained indicate to what extent present experimental data allow 3×3 CKM unitarity to be broken in these models, and are too small to be observed in the near future. As a by-product, we reproduce the calculation of these branching ratios in the SM, and with an improved set of parameters we obtain values one order of magnitude smaller than the ones usually quoted in the literature. We study the CP asymmetries between the decay rates of the top quark and antiquark, which can be much larger than in the SM, also as a consequence of the partial breaking of 3×3 CKM unitarity.

1 Introduction

The arrival of top factories, LHC and TESLA, will bring a tremendous improvement in our knowledge of top quark properties [1, 2]. In particular, the large top samples produced will allow to perform precision studies of top rare decays. In this field, flavour-changing neutral (FCN) decays $t \rightarrow cZ$, $t \rightarrow c\gamma$, $t \rightarrow cg$, deserve special attention. Within the Standard Model (SM) they are mediated at lowest order in perturbation theory by penguin diagrams with quarks of charge $Q = -1/3$ inside the loop. Due to the smallness of down-type quark masses compared to M_W , these decays are very suppressed by the GIM mechanism, in contrast with processes like $b \rightarrow s\gamma$, with diagrams with a top quark in the loop. This extra suppression results in decay rates $O(10^{-10})$ or smaller [3]. On the other hand, in several SM extensions the branching

ratios for FCN top decays can be orders of magnitude larger. For instance, in two Higgs doublet models $\text{Br}(t \rightarrow cZ) \sim 10^{-6}$, $\text{Br}(t \rightarrow c\gamma) \sim 10^{-7}$, $\text{Br}(t \rightarrow cg) \sim 10^{-5}$ can be achieved [4]. In supersymmetric models with R parity conservation these branching ratios can reach $\text{Br}(t \rightarrow cZ) \sim 10^{-6}$, $\text{Br}(t \rightarrow c\gamma) \sim 10^{-6}$, $\text{Br}(t \rightarrow cg) \sim 10^{-5}$ [5, 6].

Here we are interested in the possible enhancement of these rates in models with vector-like quark singlets. The addition of quark singlets to the SM particle content represents the simplest way to break the GIM mechanism consistently. In these models, the 3×3 Cabibbo-Kobayashi-Maskawa (CKM) matrix is not unitary, and thus FCN couplings to the Z boson appear at tree-level. FCN couplings between light quarks are experimentally constrained to be very small, but this is not the case for the top quark. Actually, top FCN vertices can mediate the decays $t \rightarrow uZ$ and $t \rightarrow cZ$, giving observable rates in models with up-type singlets [7]. The largest branching ratios allowed by present experimental data are $\text{Br}(t \rightarrow uZ) = 7.0 \times 10^{-4}$, $\text{Br}(t \rightarrow cZ) = 6.0 \times 10^{-4}$ [8], much smaller than present direct limits $\text{Br}(t \rightarrow uZ), \text{Br}(t \rightarrow cZ) \leq 0.08$ [9] but still observable at LHC [10, 11, 12] and TESLA [13, 14, 15]. In this Letter we investigate the enhancement of the branching ratios for the two other FCN decays, $t \rightarrow c\gamma$ and $t \rightarrow cg$, in the presence of either up or down singlets. We find the rates of these processes allowed by present experimental constraints, and study how the GIM suppression takes place in these models. For completeness we also quote without discussion the results for $t \rightarrow u\gamma$ and $t \rightarrow ug$, which in the SM are suppressed by the ratio $|V_{ub}/V_{cb}|^2$ with respect to the former, but in these SM extensions can have the same magnitude.

2 Overview of the Lagrangian

A full discussion of the Lagrangian in the weak eigenstate and mass eigenstate bases can be found for instance in Refs. [16, 17]. Here we only collect the terms of the Lagrangian in the mass eigenstate basis relevant for our study. We consider the SM extended with n_u up singlets and n_d down singlets, with n_u, n_d arbitrary for the moment. The charged current Lagrangian is

$$\mathcal{L}_W = -\frac{g}{\sqrt{2}} \bar{u}_L \gamma^\mu V d_L W_\mu^+ + \text{h.c.}, \quad (1)$$

with V the generalised CKM matrix, of dimension $(3 + n_u) \times (3 + n_d)$. The neutral-current Lagrangian describing the interactions with the Z boson is

$$\mathcal{L}_Z = -\frac{g}{2c_W} \left(\bar{u}_L \gamma^\mu X^u u_L - \bar{d}_L \gamma^\mu X^d d_L - 2s_W^2 J_{\text{EM}}^\mu \right) Z_\mu, \quad (2)$$

where X^u, X^d are hermitian matrices of dimension $(3+n_u) \times (3+n_u)$ and $(3+n_d) \times (3+n_d)$, respectively. These matrices can be related to the CKM matrix by $X^u = V V^\dagger$, $X^d = V^\dagger V$. The interactions with the unphysical charged scalars ϕ^\pm are given by

$$\mathcal{L}_\phi = -\frac{g}{\sqrt{2}M_W} \bar{u} (\mathcal{M}^u V P_L - V \mathcal{M}^d P_R) d \phi^+ + \text{h.c.}, \quad (3)$$

with \mathcal{M}^u and \mathcal{M}^d the diagonal mass matrices for the up and down quarks. The terms corresponding to the unphysical neutral scalar χ are

$$\begin{aligned} \mathcal{L}_\chi = & \frac{ig}{2M_W} [\bar{u} (\mathcal{M}^u X^u P_L - X^u \mathcal{M}^u P_R) u \\ & - \bar{d} (\mathcal{M}^d X^d P_L - X^d \mathcal{M}^d P_R) d] \chi. \end{aligned} \quad (4)$$

Finally, the terms describing the interactions with the Higgs boson are

$$\begin{aligned} \mathcal{L}_H = & \frac{g}{2M_W} [\bar{u} (\mathcal{M}^u X^u P_L + X^u \mathcal{M}^u P_R) u \\ & + \bar{d} (\mathcal{M}^d X^d P_L + X^d \mathcal{M}^d P_R) d] H. \end{aligned} \quad (5)$$

In our analysis of $t \rightarrow c\gamma$ and $t \rightarrow cg$ we discuss the two simplest cases: $n_u = 1$, $n_d = 0$ (which will be called Model I) and $n_u = 0$, $n_d = 1$ (Model II). These two cases correspond to CKM matrices of dimension 4×3 and 3×4 , respectively, and in both models the CKM matrix is a submatrix of a unitary 4×4 matrix.

3 Calculation of the decay rates

Using unbroken $SU(3) \times U(1)$ gauge invariance and the facts that final state particles are on-shell and the photon has transverse polarisation, the transition amplitude for $t \rightarrow c\gamma$ can be written with all generality as

$$\mathcal{M}(t \rightarrow c\gamma) = \bar{u}(p_c) [i\sigma^{\mu\nu} q_\nu (A_\gamma + B_\gamma \gamma_5)] u(p_t) \epsilon_\mu^*(q), \quad (6)$$

with p_t and p_c the momenta of the top and charm quarks, respectively, $q = p_t - p_c$ the photon momentum and ϵ its polarisation vector. This expression also assumes that the top quark is on-shell, which is an excellent approximation. A similar structure is valid for $t \rightarrow cg$, with form factors A_g and B_g . In order to compute the amplitude the form factors are written in terms of Passarino-Veltman integrals [18] using `FORM` [19]. The integrals are numerically evaluated using `LoopTools` [20]. The Feynman diagrams relevant for $t \rightarrow c\gamma$ in the SM and Model II are depicted in Fig. 1. In the

SM the down-type quarks d_i in the loops are $d_i = d, s, b$, while in Model II there is an extra heavy quark B . The contributions of these diagrams to A_γ and B_γ in the 't Hooft-Feynman gauge are collected in the Appendix. The diagrams relevant for A_g and B_g are the analogous to (1a) and (1b) in Fig. 1 but replacing the outgoing photon by a gluon.

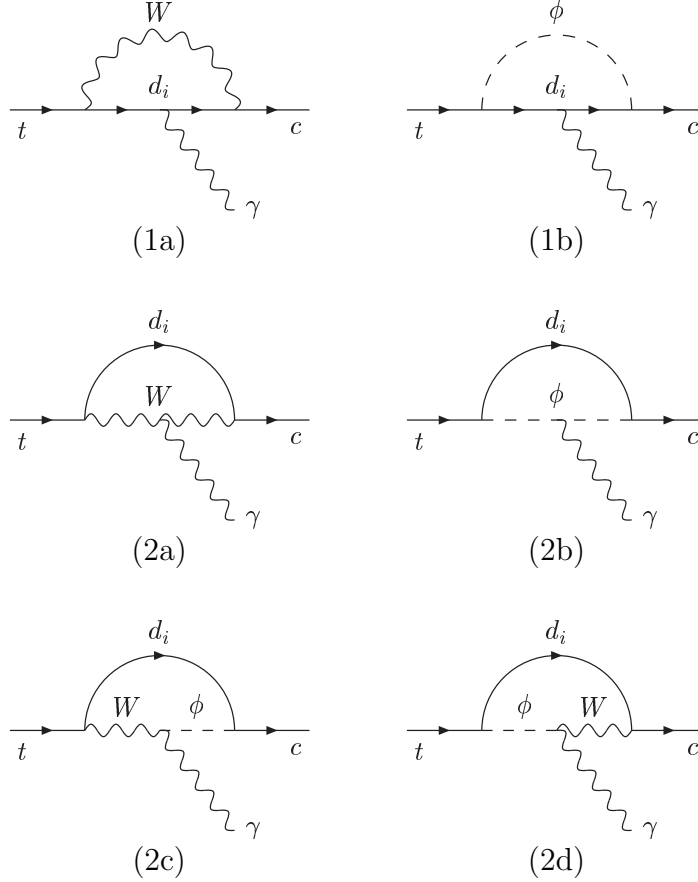


Figure 1: Feynman diagrams contributing to the $t \rightarrow c\gamma$ decay amplitude in the SM and Model II.

In Model I there are extra diagrams with up-type quarks $u_i = u, c, t, T$ in the loops (see Fig. 2). These diagrams have one FCN vertex for $u_i = c, t$ and two for $u_i = u, T$, in which case they are very suppressed. The flavour-diagonal vertices are modified with respect to the SM value. For instance, the diagonal couplings of a quark $q = u_i, d_i$ to the Z boson are

$$\begin{aligned} c_L^q &= \pm X_{qq} - 2Q_q s_W^2, \\ c_R^q &= -2Q_q s_W^2, \end{aligned} \tag{7}$$

as can be seen from Eq. (2), with the plus (minus) sign for up (down) quarks. The interactions with the unphysical scalar χ and the Higgs boson can be read from Eqs. (4,5). The contributions of these diagrams to A_γ and B_γ can be found in the Appendix.

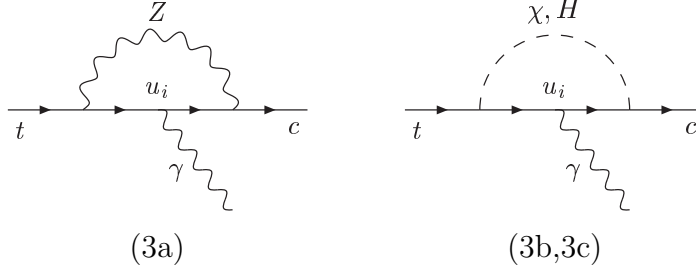


Figure 2: Additional Feynman diagrams contributing to the $t \rightarrow c\gamma$ decay amplitude in Model I. The diagrams for $t \rightarrow cg$ are similar, replacing the photon by a gluon.

We perform the computation keeping all quark masses. For external quarks we use the pole masses $m_t = 174.3$ GeV, $m_c = 1.5$ GeV. For internal quarks it is more adequate to use $\overline{\text{MS}}$ masses at a scale $O(m_t)$, rather than pole masses. This is an important difference due to the strong dependence on the b quark mass as a consequence of the GIM suppression. For a pole mass $m_b = 4.7 \pm 0.3$ GeV, $\overline{m}_b(m_t) = 2.74 \pm 0.17$ GeV [21].

In the limit $m_c = 0$ the vector and axial form factors are equal: $A_\gamma = B_\gamma$, $A_g = B_g$. Since m_c is small, $A_\gamma \simeq B_\gamma$, $A_g \simeq B_g$ and the effective couplings are predominantly right-handed. One important feature is that the form factors acquire imaginary parts from the contributions with d , s , b quarks (and u , c quarks in the extra diagrams present in Model I). These imaginary parts are one of the ingredients needed in order to have CP asymmetries $\Gamma(t \rightarrow c\gamma) \neq \Gamma(\bar{t} \rightarrow \bar{c}\gamma)$, which will be analysed in detail later.

From Eq. (6), the partial widths of these processes are

$$\begin{aligned} \Gamma(t \rightarrow c\gamma) &= \frac{1}{\pi} \left[\frac{m_t^2 - m_c^2}{2m_t} \right]^3 (|A_\gamma|^2 + |B_\gamma|^2), \\ \Gamma(t \rightarrow cg) &= \frac{C_F}{\pi} \left[\frac{m_t^2 - m_c^2}{2m_t} \right]^3 (|A_g|^2 + |B_g|^2), \end{aligned} \quad (8)$$

with $C_F = 4/3$ a colour factor. In the SM, as well as in our models, the total width is dominated by the leading decay mode $t \rightarrow bW^+$, $\Gamma(t \rightarrow bW^+) = 1.57 |V_{tb}|^2$ for $m_t = 174.3$ GeV, $M_W = 80.39$ GeV. The branching ratios are then

$$\text{Br}(t \rightarrow c\gamma) = \frac{\Gamma(t \rightarrow c\gamma)}{\Gamma(t \rightarrow bW^+)}, \quad \text{Br}(t \rightarrow cg) = \frac{\Gamma(t \rightarrow cg)}{\Gamma(t \rightarrow bW^+)}. \quad (9)$$

We do not use the next-to-leading order partial width $\Gamma(t \rightarrow bW^+) = 1.42 |V_{tb}|^2$ for consistency, because our calculation for $t \rightarrow c\gamma$, $t \rightarrow cg$ is at leading order.

We have checked that using the set of input parameters of Ref. [3] our results agree with the results presented there. For the calculation of the branching ratios within the SM we take $|V_{us}| = 0.2224$, $|V_{ub}| = 0.00362$, $|V_{cb}| = 0.0402$. These values are obtained performing a fit to the six measured CKM matrix elements, using 3×3 unitarity. The phase δ in the standard parameterisation [22] is $\delta = 1.014$, obtained with a fit to ε , ε'/ε , $a_{\psi K_S}$ and $|\delta m_B|$ (see Ref. [8]). The SM predictions are

$$\begin{aligned} \text{Br}(t \rightarrow c\gamma) &= (4.6^{+1.2}_{-1.0} \pm 0.4^{+1.6}_{-0.5}) \times 10^{-14}, \\ \text{Br}(t \rightarrow cg) &= (4.6^{+1.1}_{-0.9} \pm 0.4^{+2.1}_{-0.7}) \times 10^{-12}. \end{aligned} \quad (10)$$

The first uncertainty comes from the bottom mass, the second from CKM mixing angles and the third is estimated varying the renormalisation scale between M_Z (plus sign) and $1.5 m_t$ (minus sign). These figures are ten times smaller than the ones quoted in Ref. [3], where the pole mass is used for the internal b quark ($m_b = 5$ GeV is assumed). The uncertainty in the top mass does not affect these values, because the partial widths of $t \rightarrow c\gamma$, $t \rightarrow cg$ are proportional to m_t^3 , and the partial width of $t \rightarrow bW^+$ is approximately given by

$$\Gamma(t \rightarrow bW^+) = \frac{g^2}{64\pi} |V_{tb}|^2 \frac{m_t^3}{M_W^2} \left[1 - 3 \frac{M_W^4}{m_t^4} + 2 \frac{M_W^6}{m_t^6} \right]. \quad (11)$$

Hence, the leading dependence on m_t cancels in the ratios and the uncertainty in m_t hardly affects the numbers quoted in Eqs. (10). The SM predictions for $t \rightarrow u\gamma$ and $t \rightarrow ug$ are

$$\begin{aligned} \text{Br}(t \rightarrow u\gamma) &= (3.7^{+1.0}_{-0.8} \pm 2.1^{+1.3}_{-0.4}) \times 10^{-16}, \\ \text{Br}(t \rightarrow ug) &= (3.7^{+0.9}_{-0.8} \pm 2.1^{+1.7}_{-0.5}) \times 10^{-14}, \end{aligned} \quad (12)$$

suppressed by a factor $|V_{ub}/V_{cb}|^2 \simeq 8 \times 10^{-3}$ with respect to top decays to a charm quark. The uncertainties have the same origin as in Eqs. (10).

4 CKM unitarity and GIM suppression

Let us discuss how the GIM mechanism suppresses these processes within the SM and how this suppression can be partially removed with the addition of vector-like singlets.

We only study $t \rightarrow c\gamma$, the discussion of $t \rightarrow cg$ is formally identical. In the SM and Model II the form factors for the γtc vertex can be decomposed as

$$\begin{aligned} A_\gamma &= \sum_i f_{\gamma A}(m_i) \lambda_{ct}^i, \\ B_\gamma &= \sum_i f_{\gamma B}(m_i) \lambda_{ct}^i, \end{aligned} \quad (13)$$

where $i = 1, 2, 3$ in the SM and $i = 1 \cdots 4$ in Model II, $f_{\gamma A}(m_i)$, $f_{\gamma B}(m_i)$ are functions of the internal quark mass and $\lambda_{ct}^i = V_{ci}V_{ti}^*$ are CKM factors. We have dropped the bar over m_i , which are understood as $\overline{\text{MS}}$ masses. Since $f_{\gamma A}(m_i) \simeq f_{\gamma B}(m_i)$, we only analyse A_γ . The mass dependence of the real and imaginary parts of $f_{\gamma A}(m_i)$ is shown in Fig. 3.

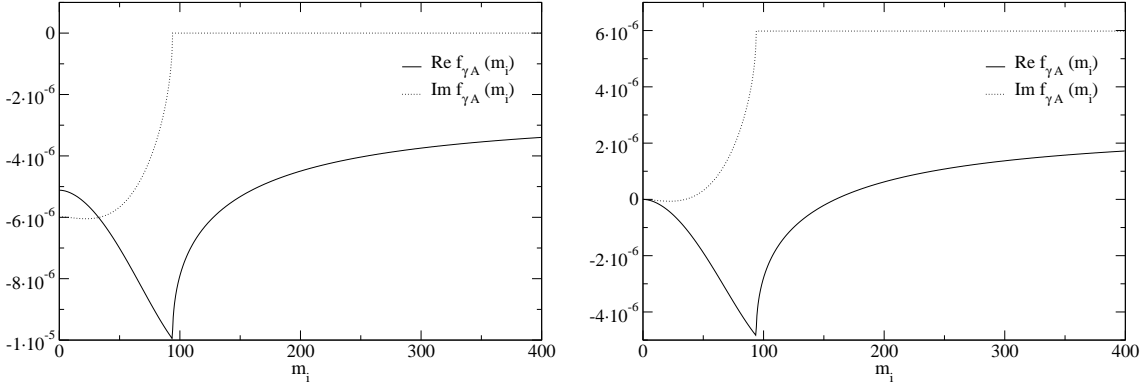


Figure 3: Loop functions $f_{\gamma A}(m_i)$ and $f'_{\gamma A}(m_i)$ for down-type internal quarks (notice the different scales).

In order to estimate the branching ratio for $t \rightarrow c\gamma$ we make the approximation $f_{\gamma A}(m_d) = f_{\gamma A}(m_s) = f_{\gamma A}(0)$ for the moment. Then, using

$$\lambda_{ct}^d + \lambda_{ct}^s + \lambda_{ct}^b + \lambda_{ct}^B = 0, \quad (14)$$

as implied by the unbroken row unitarity of the 3×4 CKM matrix V , we have

$$\begin{aligned} A_\gamma &= [f_{\gamma A}(m_b) - f_{\gamma A}(0)] \lambda_{ct}^b + [f_{\gamma A}(m_B) - f_{\gamma A}(0)] \lambda_{ct}^B \\ &\equiv f'_{\gamma A}(m_b) \lambda_{ct}^b + f'_{\gamma A}(m_B) \lambda_{ct}^B. \end{aligned} \quad (15)$$

Therefore, the decay amplitude is actually controlled by the shifted function $f'_{\gamma A}(m_i)$, plotted in Fig. 3 as well. The parameter λ_{ct}^B measures the orthogonality of the c and t rows of the 3×3 CKM submatrix $V_{3 \times 3}$ (see Eq. (14)), *i. e.* the breaking of

the GIM mechanism in this process. The SM limit is recovered setting, $\lambda_{ct}^B = 0$, so the only contribution to the form factor is given by the small function $f'_{\gamma A}(m_b) \simeq -9.1 \times 10^{-9} - 4.7 \times 10^{-9} i$ multiplied by $\lambda_{ct}^b \simeq 0.04$. With an extra down quark, there is a new term with a larger function $f'_{\gamma A}(m_B) \simeq 4.9 \times 10^{-7} + 6.0 \times 10^{-6} i$ (for $m_B = 200$ GeV), which is however suppressed by λ_{ct}^B .

The parameter λ_{ct}^B can be related to the breaking of the column unitarity of $V_{3 \times 3}$. This is easily understood, because if the columns of this submatrix are orthogonal, so must be the rows. The explicit relation can be written using the extension of the Wolfenstein parameterisation [23] in Ref. [24]. Assuming that $X_{ds}, X_{db}, X_{sb} \sim \lambda^4$, $1 - X_{ss} \sim \lambda^3$ and $1 - X_{bb} \sim \lambda^3$, we have

$$-\lambda_{ct}^B = \sum_{i=1}^3 V_{ci} V_{ti}^* = X_{sb} - \lambda X_{db} + A \lambda^2 (X_{bb} - X_{ss}) - \frac{\lambda^2}{2} X_{sb} + O(\lambda^7). \quad (16)$$

This equation shows how the breaking of the orthogonality of the first three columns of V “propagates” to the second and third rows. The effect of the new quark can be estimated with $\lambda \simeq 0.22$, $A \simeq 1$ and the typical values $X_{db} \sim 10^{-3}$, $X_{sb} \sim 10^{-3}$, $X_{bb} - X_{ss} \sim 10^{-3}$ [8], obtaining $\lambda_{ct}^B \simeq X_{sb} \sim 10^{-3}$. With this value the B contribution is 20 times larger than the b term, giving $\text{Br}(t \rightarrow c\gamma) \sim 10^{-11}$.

In Model I, neglecting for the moment diagrams with two FCN vertices, A_γ can be decomposed as

$$A_\gamma = \sum_{i=1}^3 f_{\gamma A}(m_i) \lambda_{ct}^i + g_{\gamma A} X_{ct}, \quad (17)$$

with $g_{\gamma A}$ the sum of the c and t diagram contributions, which is roughly of the same size as the $f_{\gamma A}$ functions. In this model we have the relation

$$\lambda_{ct}^d + \lambda_{ct}^s + \lambda_{ct}^b = X_{ct} \quad (18)$$

expressing the non-orthogonality of the second and third rows of the CKM matrix, of dimension 4×3 in this case (compare with Eq. (14)). Hence, the form factor is written as

$$\begin{aligned} A_\gamma &= [f_{\gamma A}(m_b) - f_{\gamma A}(0)] \lambda_{ct}^b + [g_{\gamma A} + f_{\gamma A}(0)] X_{ct} \\ &\equiv f'_{\gamma A}(m_b) \lambda_{ct}^b + g'_{\gamma A} X_{ct}, \end{aligned} \quad (19)$$

with $g'_{\gamma A} = -4.4 \times 10^{-6} - 4.8 \times 10^{-6} i$. In this model the FCN coupling X_{ct} can be $X_{ct} \sim 0.04$ for $V_{tb} \sim 0.6$ [8], yielding a branching ratio $\text{Br}(t \rightarrow c\gamma) \sim 5 \times 10^{-8}$.

We note that the larger branching ratio achieved in Model I is *not* a consequence of the presence of a tree-level coupling Ztc , which appears in the expressions of the form

factors on the same footing as the parameter λ_{ct}^B . Moreover, the loop integrals of the new physics contributions of Model I, $g'_{\gamma A} = -4.4 \times 10^{-6} - 4.8 \times 10^{-6} i$ and of Model II, $f'_{\gamma A}(m_B) \simeq 4.9 \times 10^{-7} + 6.0 \times 10^{-6} i$, are very similar. The only reason for the larger branching ratio in Model I is that $X_{ct} \gg \lambda_{ct}^B$, that is, unitarity of $V_{3 \times 3}$ can be broken to a lesser extent in Model II due to the strong requirements on FCN couplings between light quarks. Additionally, V_{tb} can be smaller in Model I, and the total top width is reduced.

We are also interested in the CP asymmetry

$$a_\gamma = \frac{\Gamma(t \rightarrow c\gamma) - \Gamma(\bar{t} \rightarrow \bar{c}\gamma)}{\Gamma(t \rightarrow c\gamma) + \Gamma(\bar{t} \rightarrow \bar{c}\gamma)}. \quad (20)$$

This interest is mainly academic, because if the branching ratios are unobservable, even less are the asymmetries. However, the latter show how large CP asymmetries at high energy are possible in these SM extensions. Here we analyse in detail a_γ in Model II, the results for Model I are similar but more involved. The form factors for $\bar{t} \rightarrow \bar{c}\gamma$ are

$$\bar{A}_\gamma = f'_{\gamma A}(m_b)\lambda_{ct}^{b*} + f'_{\gamma A}(m_B)\lambda_{ct}^{B*}, \quad (21)$$

and an analogous expression for \bar{B}_γ . The asymmetry can be written as $a_\gamma = N_\gamma/D_\gamma$, with

$$\begin{aligned} N_\gamma &= -2 \operatorname{Im} \left[f'_{\gamma A}(m_b)f'_{\gamma A}(m_B) + f'_{\gamma B}(m_b)f'_{\gamma B}(m_B) \right] \operatorname{Im} \left[\lambda_{ct}^b \lambda_{ct}^{B*} \right] \\ D_\gamma &= \left[|f'_{\gamma A}(m_b)|^2 + |f'_{\gamma B}(m_b)|^2 \right] |\lambda_{ct}^b|^2 + \left[|f'_{\gamma A}(m_B)|^2 + |f'_{\gamma B}(m_B)|^2 \right] |\lambda_{ct}^{B*}|^2 \\ &\quad + 2 \operatorname{Re} \left[f'_{\gamma A}(m_b)f'_{\gamma A}(m_B) + f'_{\gamma B}(m_b)f'_{\gamma B}(m_B) \right] \operatorname{Re} \left[\lambda_{ct}^b \lambda_{ct}^{B*} \right]. \end{aligned} \quad (22)$$

A few comments are in order:

1. The CP asymmetry a_γ is proportional to the imaginary part of the rephasing-invariant quartet $\lambda_{ct}^b \lambda_{ct}^{B*} = V_{cb}V_{cB}^*V_{tb}^*V_{tB}$. This is expected from general grounds. In fact, it can be shown that in a model with an extra down singlet *all* CP violating observables at high energy (that is, when $m_{u,d,s} \sim 0$ compared to the scale of energy involved) must be proportional to $\operatorname{Im} V_{cb}V_{cB}^*V_{tb}^*V_{tB}$, $\operatorname{Im} V_{cb}V_{cB}^*X_{bB}$, $\operatorname{Im} V_{tb}V_{tB}^*X_{bB}$, or a combination of them [25].
2. The SM limit is recovered setting $\lambda_{ct}^B = 0$, obtaining a vanishing CP asymmetry. It is a well-known fact that CP asymmetries at high energy are very small in the SM, due to the smallness of m_u , m_d and m_s and the fact that u, d, s jets cannot be distinguished. When all the quark masses are kept in the computation

a non-vanishing but a negligible asymmetry $a_\gamma \sim -6 \times 10^{-6}$ is obtained. For the gluon case, the asymmetry $a_g \sim -5 \times 10^{-6}$ is also extremely small.

3. The large phases in the functions $f'_{\gamma A}$, $f'_{\gamma B}$ allow to obtain relatively large CP asymmetries, provided $\text{Im} \lambda_{ct}^b \lambda_{ct}^{B*}$ is sizeable.

5 Results

We explore the parameter space of Models I and II to find the maximum values of $\text{Br}(t \rightarrow c\gamma)$ and $\text{Br}(t \rightarrow cg)$ allowed by present experimental measurements. The constraints on these models come from precision electroweak data, K and B physics and atomic parity violation (the details of the analysis can be found in Ref. [8]). We take all the quark masses into account, and require that the mass of the new quark is larger than 200 GeV to satisfy the limits from direct searches. In Model I, assuming that the new quark has a mass $m_T = 200$ GeV, we find the maximum rates

$$\begin{aligned} \text{Br}(t \rightarrow c\gamma) &= 4.5 \times 10^{-8}, \\ \text{Br}(t \rightarrow cg) &= 8.9 \times 10^{-7}, \end{aligned} \tag{23}$$

corresponding to $|X_{ct}| = 0.037$, $|V_{tb}| = 0.58$. (The branching ratios scale with $|X_{ct}|^2$ approximately.) For larger m_T , the allowed values of $|X_{ct}|$ are smaller [8], and these branching ratios decrease. The CP asymmetries corresponding to the figures in Eqs. (23) are negligible,

$$\begin{aligned} a_\gamma &= -0.0006, \\ a_g &= -0.002, \end{aligned} \tag{24}$$

because the rates are dominated by the X_{ct} term. The asymmetries can have values in the range $-0.5 \leq a_\gamma \leq 0.4$, $-0.9 \leq a_g \leq 0.6$, but only reach the boundaries of these intervals for branching ratios much smaller than those in Eqs. (23). The results for decays to up quarks are a little larger,

$$\begin{aligned} \text{Br}(t \rightarrow u\gamma) &= 4.6 \times 10^{-8}, \\ \text{Br}(t \rightarrow ug) &= 9.2 \times 10^{-7}. \end{aligned} \tag{25}$$

In Model II, assuming that the mass of the new quark is $m_B = 200$ GeV, we have

$$\begin{aligned} \text{Br}(t \rightarrow c\gamma) &= 4.5 \times 10^{-12}, \\ \text{Br}(t \rightarrow cg) &= 6.6 \times 10^{-11}. \end{aligned} \tag{26}$$

These numbers are almost insensitive to the mass of the new $Q = -1/3$ quark for $m_B \geq 200$ GeV, as can be seen from Fig. 1, and show a small increase with m_B . The corresponding asymmetries are

$$\begin{aligned} a_\gamma &= -0.05, \\ a_g &= 0.56. \end{aligned} \tag{27}$$

In general, the CP asymmetries take values in the intervals $-1 \leq a_\gamma \leq 1$, $-1 \leq a_g \leq 1$. The decay rates to up quarks are larger,

$$\begin{aligned} \text{Br}(t \rightarrow u\gamma) &= 7.4 \times 10^{-12}, \\ \text{Br}(t \rightarrow ug) &= 9.5 \times 10^{-11}. \end{aligned} \tag{28}$$

The branching ratios in Eqs. (23–28) are too small to be measurable in the near future. The estimated 3σ sensitivities of LHC to these decays are $\text{Br}(t \rightarrow c\gamma) = 1.2 \times 10^{-5}$ [26], $\text{Br}(t \rightarrow u\gamma) = 3.0 \times 10^{-6}$ [12], $\text{Br}(t \rightarrow cg) = 2.7 \times 10^{-5}$ and $\text{Br}(t \rightarrow ug) = 4.1 \times 10^{-6}$ [27], with an integrated luminosity of 100 fb^{-1} . The TESLA sensitivity to $t \rightarrow c\gamma$ is better but not enough, $\text{Br}(t \rightarrow c\gamma) = 3.6 \times 10^{-6}$ [14] with a centre of mass energy of 800 GeV and a luminosity of 500 fb^{-1} . Hence, we observe that in models with up-type singlets the rates for $t \rightarrow qZ$, $q = u, c$ can be observable but not the rates for $t \rightarrow q\gamma$ and $t \rightarrow qg$, which are four and three orders of magnitude smaller, respectively. This fact contrasts with the results for two Higgs doublet models or supersymmetric extensions of the SM, where the branching ratios for $t \rightarrow cZ$ and $t \rightarrow c\gamma$ are similar, and the branching ratio for $t \rightarrow cg$ is one order of magnitude larger. This difference would allow for a consistency check of the models, should a positive signal of top FCN decays be discovered.

Acknowledgements

J.A.A.S. thanks F. del Águila and M. Pérez-Victoria for comments and discussions. B.M.N. thanks D.F. Carvalho for useful discussions. We thank F. del Águila and G.C. Branco for reading of the manuscript. This work has been supported by the European Community's Human Potential Programme under contract HTRN-CT-2000-00149 Physics at Colliders and by FCT through project CERN/FIS/43793/2001. The work of B.M.N. has been supported by FCT under the grant SFRH/BD/995/2000.

A Form factors for $t \rightarrow c\gamma$ and $t \rightarrow cg$

The contributions to A_γ and B_γ of diagrams (1a) and (1b) with an internal quark d_i are

$$A_{\gamma,1a} = -\frac{Q_i g^2 e}{2} \frac{1}{16\pi^2} V_{2i} V_{3i}^* \{ (m_t + m_c) C_0 + (2m_t + m_c) C_1 + (m_t + 2m_c) C_2 + m_t C_{11} + (m_t + m_c) C_{12} + m_c C_{22} \}, \quad (29)$$

$$B_{\gamma,1a} = -\frac{Q_i g^2 e}{2} \frac{1}{16\pi^2} V_{2i} V_{3i}^* \{ (m_t - m_c) C_0 + (2m_t - m_c) C_1 + (m_t - 2m_c) C_2 + m_t C_{11} + (m_t - m_c) C_{12} - m_c C_{22} \}, \quad (30)$$

$$A_{\gamma,1b} = -\frac{Q_i g^2 e}{4M_W^2} \frac{1}{16\pi^2} V_{2i} V_{3i}^* \{ m_c(m_t^2 - \bar{m}_{d_i}^2) C_1 + m_t(m_c^2 - \bar{m}_{d_i}^2) C_2 + (m_t \bar{m}_{d_i}^2 + m_c m_t^2) C_{11} + [m_t(m_c^2 + \bar{m}_{d_i}^2) + m_c(m_t^2 + \bar{m}_{d_i}^2)] C_{12} + (m_t m_c^2 + m_c \bar{m}_{d_i}^2) C_{22} \}, \quad (31)$$

$$B_{\gamma,1b} = -\frac{Q_i g^2 e}{4M_W^2} \frac{1}{16\pi^2} V_{2i} V_{3i}^* \{ -m_c(m_t^2 - \bar{m}_{d_i}^2) C_1 + m_t(m_c^2 - \bar{m}_{d_i}^2) C_2 + (m_t \bar{m}_{d_i}^2 - m_c m_t^2) C_{11} + [m_t(m_c^2 + \bar{m}_{d_i}^2) - m_c(m_t^2 + \bar{m}_{d_i}^2)] C_{12} + (m_t m_c^2 - m_c \bar{m}_{d_i}^2) C_{22} \}. \quad (32)$$

The C 's are functions of the external and internal masses, $C(m_t^2, 0, m_c^2, M_W^2, \bar{m}_{d_i}^2, \bar{m}_{d_i}^2)$ in the notation of Ref. [20]. For $t \rightarrow cg$ the contributions to the form factors A_g and B_g can be obtained replacing e by g_s and setting $Q_i = 1$ in Eqs. (29–32). The terms from diagrams (2a)–(2d) are

$$A_{\gamma,2a} = \frac{g^2 e}{4} \frac{1}{16\pi^2} V_{2i} V_{3i}^* \{ (2m_t + m_c) C_0 + (4m_t + m_c) C_1 + (m_t - m_c) C_2 + 2m_t C_{11} + 2(m_t - m_c) C_{12} \}, \quad (33)$$

$$B_{\gamma,2a} = \frac{g^2 e}{4} \frac{1}{16\pi^2} V_{2i} V_{3i}^* \{ (2m_t - m_c) C_0 + (4m_t - m_c) C_1 + (m_t + m_c) C_2 + 2m_t C_{11} + 2(m_t + m_c) C_{12} \}, \quad (34)$$

$$A_{\gamma,2b} = \frac{g^2 e}{4M_W^2} \frac{1}{16\pi^2} V_{2i} V_{3i}^* \{ m_c(m_t^2 - \bar{m}_{d_i}^2) C_1 + (m_t \bar{m}_{d_i}^2 + m_c m_t^2) C_{11} + [m_t(\bar{m}_{d_i}^2 - m_c^2) + m_c(m_t^2 - \bar{m}_{d_i}^2)] C_{12} \}, \quad (35)$$

$$B_{\gamma,2b} = \frac{g^2 e}{4M_W^2} \frac{1}{16\pi^2} V_{2i} V_{3i}^* \{ -m_c(m_t^2 - \bar{m}_{d_i}^2) C_1 + (m_t \bar{m}_{d_i}^2 - m_c m_t^2) C_{11} + [m_t(\bar{m}_{d_i}^2 - m_c^2) - m_c(m_t^2 - \bar{m}_{d_i}^2)] C_{12} \}, \quad (36)$$

$$A_{\gamma,2c} = \frac{g^2 e}{4} \frac{1}{16\pi^2} V_{2i} V_{3i}^* \{ m_c C_0 + m_c C_1 + m_c C_2 \}, \quad (37)$$

$$B_{\gamma,2c} = \frac{g^2 e}{4} \frac{1}{16\pi^2} V_{2i} V_{3i}^* \{-m_c C_0 - m_c C_1 - m_c C_2\}, \quad (38)$$

$$A_{\gamma,2d} = \frac{g^2 e}{4} \frac{1}{16\pi^2} V_{2i} V_{3i}^* \{-m_t C_2\}, \quad (39)$$

$$B_{\gamma,2d} = \frac{g^2 e}{4} \frac{1}{16\pi^2} V_{2i} V_{3i}^* \{-m_t C_2\}. \quad (40)$$

Here the arguments of the functions are $C(m_t^2, m_c^2, 0, M_W^2, \overline{m}_{d_i}^2, M_W^2)$. In Model I the contributions from diagrams (3a) and (3b) with internal quarks u_i are

$$\begin{aligned} A_{\gamma,3a} &= \frac{Q_i g^2 e}{4c_W^2} \frac{1}{16\pi^2} \left\{ c_{LL}^i [-(m_t + m_c) C_0 - (2m_t + m_c) C_1 - (m_t + 2m_c) C_2 \right. \\ &\quad \left. - m_t C_{11} - (m_t + m_c) C_{12} - m_c C_{22}] + (c_{LR}^i + c_{RL}^i) 2\overline{m}_{u_i} [C_0 + C_1 + C_2] \right\}, \\ B_{\gamma,3a} &= \frac{Q_i g^2 e}{4c_W^2} \frac{1}{16\pi^2} \left\{ c_{LL}^i [-(m_t - m_c) C_0 - (2m_t - m_c) C_1 - (m_t - 2m_c) C_2 \right. \\ &\quad \left. - m_t C_{11} - (m_t - m_c) C_{12} + m_c C_{22}] + (c_{LR}^i - c_{RL}^i) 2\overline{m}_{u_i} [C_0 + C_1 + C_2] \right\}, \\ A_{\gamma,3b} &= \frac{Q_i g^2 e}{8M_W^2} \frac{1}{16\pi^2} X_{2i}^u X_{i3}^u \left\{ -m_c(m_t^2 - \overline{m}_{u_i}^2) C_1 + m_t(\overline{m}_{u_i}^2 - m_c^2) C_2 \right. \\ &\quad \left. - (m_t \overline{m}_{u_i}^2 + m_c m_t^2) C_{11} - [m_t(m_c^2 + \overline{m}_{u_i}^2) + m_c(m_t^2 + \overline{m}_{u_i}^2)] C_{12} \right. \\ &\quad \left. - (m_t m_c^2 + m_c \overline{m}_{u_i}^2) C_{22} \right\}, \end{aligned} \quad (41)$$

$$\begin{aligned} B_{\gamma,3b} &= \frac{Q_i g^2 e}{8M_W^2} \frac{1}{16\pi^2} X_{2i}^u X_{i3}^u \left\{ +m_c(m_t^2 - \overline{m}_{u_i}^2) C_1 + m_t(\overline{m}_{u_i}^2 - m_c^2) C_2 \right. \\ &\quad \left. - (m_t \overline{m}_{u_i}^2 - m_c m_t^2) C_{11} - [m_t(m_c^2 + \overline{m}_{u_i}^2) - m_c(m_t^2 + \overline{m}_{u_i}^2)] C_{12} \right. \\ &\quad \left. - (m_t m_c^2 - m_c \overline{m}_{u_i}^2) C_{22} \right\}. \end{aligned} \quad (42)$$

The constants c_{LL}^i , c_{LR}^i and c_{RL}^i are products of left-handed and right-handed couplings between (c, i) and (i, t) ,

$$\begin{aligned} c_{LL}^i &= \left(X_{ci}^u - \delta_{ci} \frac{4}{3} s_W^2 \right) \left(X_{it}^u - \delta_{it} \frac{4}{3} s_W^2 \right), \\ c_{LR}^i &= \left(X_{ci}^u - \delta_{ci} \frac{4}{3} s_W^2 \right) \left(-\delta_{it} \frac{4}{3} s_W^2 \right), \\ c_{RL}^i &= \left(-\delta_{ci} \frac{4}{3} s_W^2 \right) \left(X_{it}^u - \delta_{it} \frac{4}{3} s_W^2 \right), \end{aligned} \quad (43)$$

with $\delta_{ij} = 1$ if $i = j$ and zero otherwise. For these diagrams the arguments of the functions are $C(m_t^2, 0, m_c^2, M_Z^2, \overline{m}_{u_i}^2, \overline{m}_{u_i}^2)$. Finally, the Higgs contribution in diagram (3c) reads

$$A_{\gamma,3c} = -\frac{Q_i g^2 e}{8M_W^2} \frac{1}{16\pi^2} X_{2i}^u X_{i3}^u \left\{ [2m_t \overline{m}_{u_i}^2 + m_c(m_t^2 + \overline{m}_{u_i}^2)] C_1 \right.$$

$$\begin{aligned}
& + \left[m_t(m_c^2 + \overline{m}_{u_i}^2) + 2m_c\overline{m}_{u_i}^2 \right] C_2 + (m_t\overline{m}_{u_i}^2 + m_cm_t^2) C_{11} \\
& + \left[m_t(m_c^2 + \overline{m}_{u_i}^2) + m_c(m_t^2 + \overline{m}_{u_i}^2) \right] C_{12} + (m_tm_c^2 + m_c\overline{m}_{u_i}^2) C_{22} \} , \quad (44) \\
B_{\gamma,3c} = & -\frac{Q_i g^2 e}{8M_W^2} \frac{1}{16\pi^2} X_{2i}^u X_{i3}^u \left\{ \left[2m_t\overline{m}_{u_i}^2 - m_c(m_t^2 + \overline{m}_{u_i}^2) \right] C_1 \right. \\
& + \left[m_t(m_c^2 + \overline{m}_{u_i}^2) - 2m_c\overline{m}_{u_i}^2 \right] C_2 + (m_t\overline{m}_{u_i}^2 - m_cm_t^2) C_{11} \\
& \left. + \left[m_t(m_c^2 + \overline{m}_{u_i}^2) - m_c(m_t^2 + \overline{m}_{u_i}^2) \right] C_{12} + (m_tm_c^2 - m_c\overline{m}_{u_i}^2) C_{22} \right\} , \quad (45)
\end{aligned}$$

where the functions are $C(m_t^2, 0, m_c^2, M_H^2, \overline{m}_{u_i}^2, \overline{m}_{u_i}^2)$. We take $M_H = 115$ GeV. For $t \rightarrow cg$ the extra contributions in Model I can be obtained replacing e by g_s and setting $Q_i = 1$.

References

- [1] M. Beneke *et al.*, hep-ph/0003033
- [2] J. A. Aguilar-Saavedra *et al.* [ECFA/DESY LC Physics Working Group Collaboration], hep-ph/0106315
- [3] G. Eilam, J. L. Hewett and A. Soni, Phys. Rev. **D44** (1991) 1473 [Erratum-ibid. **D59** (1999) 039901]; J. L. Hewett, T. Takeuchi and S. Thomas, in ‘‘Electroweak Symmetry Breaking and Beyond the Standard Model’’, ed. T. Barklow *et al.*, World Scientific 1996
- [4] D. Atwood, L. Reina and A. Soni, Phys. Rev. **D55** (1997) 3156
- [5] G. M. de Divitiis, R. Petronzio and L. Silvestrini, Nucl. Phys. **B504** (1997) 45
- [6] J. L. Lopez, D. V. Nanopoulos and R. Rangarajan, Phys. Rev. **D56** (1997) 3100
- [7] F. del Aguila, J. A. Aguilar-Saavedra and R. Miquel, Phys. Rev. Lett. **82** (1999) 1628
- [8] J. A. Aguilar-Saavedra, hep-ph/0210112
- [9] G. Abbiendi *et al.* [OPAL Collaboration], Phys. Lett. **B521** (2001) 181
- [10] T. Han, R. D. Peccei and X. Zhang, Nucl. Phys. **B454** (1995) 527

- [11] F. del Aguila, J. A. Aguilar-Saavedra and Ll. Ametller, Phys. Lett. **B462** (1999) 310
- [12] F. del Aguila and J. A. Aguilar-Saavedra, Nucl. Phys. **B576** (2000) 56
- [13] T. Han and J. L. Hewett, Phys. Rev. **D60** (1999) 074015
- [14] J. A. Aguilar-Saavedra, Phys. Lett. **B502** (2001) 115
- [15] J.-j. Cao, Z.-h. Xiong and J. M. Yang, hep-ph/0208035
- [16] F. del Aguila and M. J. Bowick, Nucl. Phys. **B224** (1983) 107
- [17] G. C. Branco and L. Lavoura, Nucl. Phys. **B278** (1986) 738
- [18] G. Passarino and M. J. Veltman, Nucl. Phys. **B160** (1979) 151
- [19] J. A. Vermaseren, math-ph/0010025
- [20] T. Hahn and M. Pérez-Victoria, Comput. Phys. Commun. **118** (1999) 153
- [21] H. Fusaoka and Y. Koide, Phys. Rev. **D57** (1998) 3986
- [22] K. Hagiwara *et al.*, Particle Data Group, Phys. Rev. **D66** (2002) 010001
- [23] L. Wolfenstein, Phys. Rev. Lett. **51** (1983) 1945
- [24] G. Barenboim, F. J. Botella and O. Vives, Nucl. Phys. **B613** (2001) 285
- [25] F. del Aguila, J. A. Aguilar-Saavedra and G. C. Branco, Nucl. Phys. **B510** (1998) 39
- [26] T. Han, K. Whisnant, B.-L. Young and X. Zhang, Phys. Rev. **D55** (1997) 7241
- [27] M. Hosch, K. Whisnant and B.-L. Young, Phys. Rev. **D56** (1997) 5725